

ANALYSIS OF THE SCATTERING CHARACTERISTICS FROM DISCONTINUITY SURFACES ON AIRCRAFT USING A MODIFIED MLFMA

LIU Zhanhe*, HUANG Peilin*, WANG Zhongjie*

* School of Aeronautics Science and Technology, Beijing University of Aeronautics and Astronautics 513#, Beijing 100083, China

Keywords: MLFMA, RCS, aircraft

Abstract

The experimental and calculational curves were compared from a multi-gap plate, to validate this developed program which used MLFMA (Multilevel Fast Multipole Algorithm) can investigate the scattering from discrete character in aircraft surface. When the incoming frequency is greater, numerical results show that the electromagnetic scattering enhances and the RCS(Radar Cross Section) arithmetic average increases for single-gap, multi-gap, single-step and multi-step plates; for single-gap plate, the curves are similar for different frequencies and the second crest of curve moves far away from the major crest while the curves of single-step plate are symmetrical weakly, scattering from multi-gap and multi-step plates has coupling performance and the curves change sharply beside the characteristic of single-gap or single-step plate, the second crest of the curves moves near to the major plate for multi-step plate. This conclusion can find its application to improve the stealth performance of aircraft.

1 Numerical Calculation

1.1 Integral Equation

Normally aircrafts could be taken as metal scattering objects, thus it is only necessary to research the surface integral equation of metal objects. Assuming medium constant is ϵ and μ .

Combined Field Integral Equation (CFIE) actually is the liner combination of Electric Field Integral Equation (EFIE) and Magnetic

Field Integral Equation (MFIE). It could be used to accelerate convergence and to solve the stability and constringency problem efficiently when it is in resonance region. It may be represented as:

$$\begin{aligned} & \alpha \hat{n} \cdot \int_S dS [J(r') + \frac{1}{k^2} \nabla \cdot \nabla J(r')] g(r, r') \\ & + 2\pi \frac{i}{k} (1-\alpha) J(r) - \hat{n} \times \nabla \times \int_S dS g(r, r') J(r') \\ & = \alpha \frac{4\pi i}{k\eta} \hat{t} \cdot E^{inc}(r) + \frac{i}{k} (1-\alpha) 4\pi \hat{n} \times H^{inc}(r), r \in S \end{aligned} \quad (1)$$

where \hat{t} is random unit tangential component of the object surface, \hat{n} is unit normal component. The surface current density $J(r')$ on the left side of the equation is an unknown variable, on the right side are the inducing term $E^{inc}(r)$ which include the known incoming electric field, the inducing term $H^{inc}(r)$ of incoming magnetic field, the scalar green function $g(r, r') = e^{jk|r-r'|} / |r-r'|$. α is the factor of Combined Field Integral Equation, it could be taken as any value between 0 to 1 according to the actual situation.

After accurate geometrical modeling, plate triangle grids are used to simulate. The side length of these triangles are taken from 1/5 to 1/10, using RWG function[1] which is basing on triangle patch, the combined integral equation would be transferred into liner algebra equations set, then Multilevel Fast Multipole Method could be used to evaluate.

1.2 Statement on MLFMA of the modified truncation number L

MLFMA[2,3] has been used to accelerate the method of moments (MOM) and is the implementation of FMM (Fast Multipole

Method) in oct-tree structure. An oct-tree is created in which a large cube enclosing the entire scattering object is partitioned to smaller cubes. Each sub-cube is recursively divided into eight small cubes until the edge length of cube is about half of a wavelength. Some cubes are pruned because of empty. The number of translations can be reduced by aggregating radiation patterns that are translated to large-size cubes from smaller cubes to larger cubes in the upward pass and disaggregating is employed in the downward pass.

During the above two pass, multipole expansions is applied by interpolation and antepolation of translation, so the number of the truncation number L is required to accurately represent the spectral contents of both translation and the related radiation and receiving patterns. Previous researches applied the excess bandwidth formula as follows[4]:

$$L = kD_{\max} + 1.8(d_0)^{2/3}(kD_{\max})^{1/3} \quad (2)$$

In which D_{\max} is the largest length of cube and equal to $\sqrt{3}d$ (d is the cube edge length) commonly, d_0 is the desired accuracy. The L is doubled from the finer level to its upper level in the original method which could result in a large number of samples for integral. We employ the formula (2) in every level and d_0 is changed with different level in order to improve the result until its cube edge length is larger than 4λ , where λ is the wavelength, then the RAM and CPU time are reduced greatly, which are proved by the following numerical example and the desired accuracy is gained. the bistatic RCS example of a metallic sphere shows that 1.3GB RAM was taken and the CPU time was 43388 seconds for original method while only 457.7MB RAM was taken and the CPU time was correspondingly reduced to 8246 seconds for the modified method.

2 Experimentation on multi-gaps to prove numerical method

Discrete character, such as gaps and steps, is significant for designing and analyzing of stealth aircraft. But its scattering characteristic can not be calculated with high frequency

methods. Multi-gaps takes the most situations of discrete character and its scattering characteristic is quite complicate, so it is necessary to research it in detail. To prove the numerical method, single station RCS of plate which contain three gaps has been calculated. Fig.1 is the exact structure of three-gap plate. Side length is 400mm, depth is 5mm, the three gaps are in the centre of the plate and are parallel to its diagonal line, interval of the gap $d=30\text{mm}$ and its length is 400mm, calculation and experimentation are both change with its different pitching angle. For convenient, suppose the length of plate's diagonal line to be L , define: $R = L/\lambda$; suppose interval of three gaps/steps to be d , define: $D = d/\lambda$.

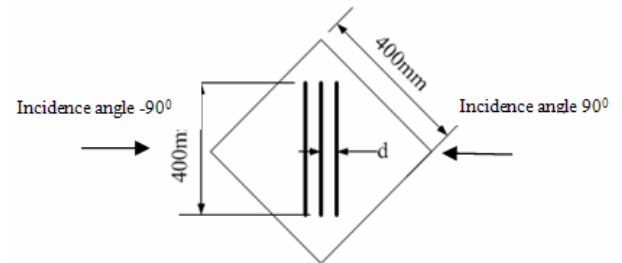


Fig.1 Exact structure of three-gaps plate

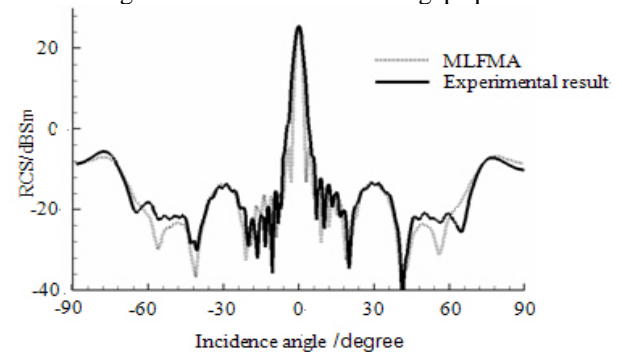


Fig.2 Comparison of calculating and experimentation of the RCS of three-gaps plate/HH polarization

Fig.2 is the curves of single station RCS of three-gaps plate when its pitching angle changes with the time, and the incoming frequency $f = 10\text{GHz}$. The curves are separately the result of experimentation and MLFMA method. When defining geometrical grids, side length of triangle patches was controlled to be $1/6$ of wavelength, used memory is 368MB, unknown number $N=46035$, side length of cube of the finest layer $D_{\text{cube}} = \lambda/2$, the combined parameter of combined integral field $\alpha = 0.5$. In equation 6, the precision is controlled as $d_0=2$, panel node number of Lagrange interpolation in the course of aggregation and disaggregation is 6×6 . In

figuration 2, the error of the both results of calculating and experimentation is $RMS_{error}=0.433dB$, which means the procedures in this paper could be used to calculate and analyze the RCS of complicate scattering targets. The unsymmetrical of the experimentation curve is cause by two reasons: three gaps are not exact symmetrical to the plate diagonal line, gaps are not exact vertical to the plate surface when they are manufactured. Because laws of the RCS curves of gaps and steps when under VV polarization condition are similar to that of HH polarization, only HH polarization situation is discussed in this paper, all the incoming frequency is 10GHz.

3 Analysis of gap scattering characteristic

3.1 Numerical calculating result of single gap

The calculation model of single gap is similar to that of three gaps. Its side length is 200mm, length of single gap is 200mm, the way to arrange the position of single gap is also the same of three gaps which is land in the direction of diagonal line. Corresponding $R=9$, so it is in the resonance region, depth of plate is 5mm, width of single gap a are separately 1mm, 3mm, 5mm, 8mm, 12mm, 16mm. Laws of influence that width of single gap a makes to its RCS curve are the main research target.

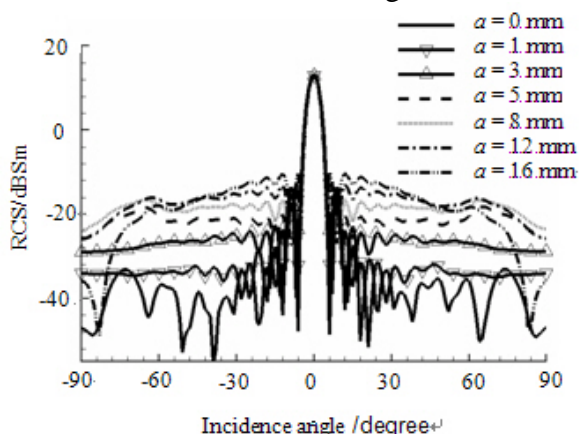


Fig. 3 Calculating RCS curves of different width of single gap

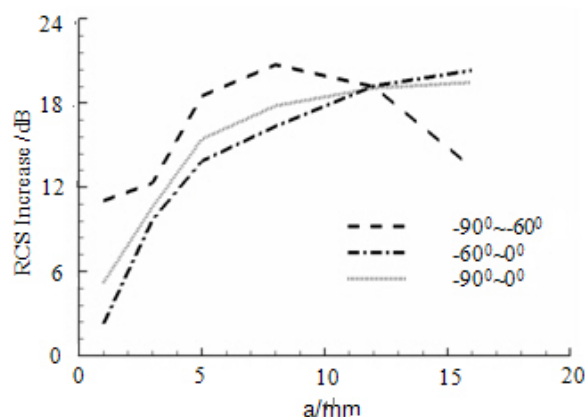


Fig. 4 RCS increase in different angle zone when width of single gap changes

Fig.3 is RCS curves of different width of single gap when their pitching angles to incoming wave change with time. Figuration 4 exhibits the RCS acceleration of different width single-gap plates comparing to flat plate in following different angle zone: $-90^{\circ}\sim-60^{\circ}$ 、 $-60^{\circ}\sim-90^{\circ}$ 、 $-90^{\circ}\sim0^{\circ}$.

It can be told from Fig.3 that the scattering of single gap is obviously stronger than plate which has no gap ($a=0mm$ means no gap on plate in figuration). When the depth of single gap increases, the increment of single gap scattering is steady in the $-60^{\circ}\sim60^{\circ}$ angle zone, which means except the mirror scattering near the 90° angle zone, the scattering curves become flat and gradually increase when width increase; in $-90^{\circ}\sim-60^{\circ}$ and $60^{\circ}\sim90^{\circ}$ angle zone, scattering curves go up at first, when $a=12mm$, it decrease fractionally, when $a=16mm$, scattering curve decrease in a great degree. In extensive incoming angle zone ($-60^{\circ}\sim60^{\circ}$), scattering level are quite close, when $a=1, 3mm$, curves are flat in the outside area of $\pm 30^{\circ}$, when $a=5, 8, 12mm$, peak value of curves appears at the nearby of $\pm 70^{\circ}$, it is the effect of the traveling wave scattering.

After analyzing figuration 4, refer to all direction scattering in $-90^{\circ}\sim90^{\circ}$, when width of single gap is less than 1/4 of wave (30mm), which means $a=1, 3, 5mm$, the increment of width lead to a fast increasing of gap scattering; when width of single gap is lager than 1/4 of wave, which means $a=8, 12, 16mm$, the increasing of gap scattering which is caused by the increment of width becomes gently, the curves tend to steady in the mass.

Refer to the surface wave scattering in the $-60^{\circ}\sim 60^{\circ}$ angle zone which is caused by single gap, when width of single gap is less than $1/4$ of wave, the increment of width would lead to the rapid increasing of surface wave scattering; when width of single gap is larger than $1/4$ of wave, the increasing of surface wave scattering which is caused by the increment of width show a downtrend.

3.2 Numerical calculating result of three gaps

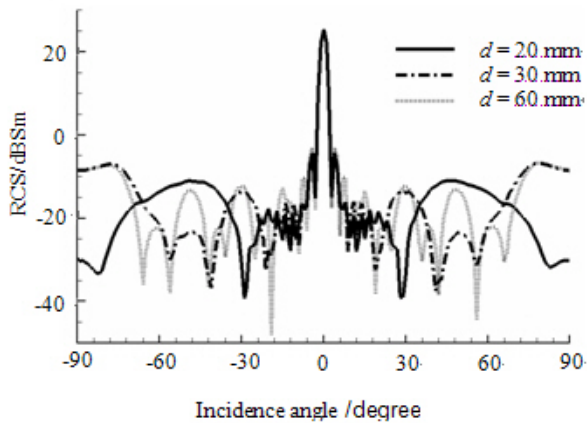


Fig. 5 Calculating RCS curves of three gaps in different gap interval situation

The exact structure of three-gap plate is as Fig.1, correspondingly $R=19$, it is in the high frequency region, Fig.5 shows the calculating RCS curves of three-gap plate when separately $d=20, 30, 60\text{mm}$, correspondingly $D=0.6, 1, 2$, it could be told from this result that gaps influent the scattering relatively more, the curves surge at the nearby of 20dBsm , refer to $d=20\text{mm}$, scattering curve is diagonal and there are two peak values, when $d=30\text{mm}$ and $d=60\text{mm}$, the number of curve peaks increases correspondingly; influence of scattering behaves that surging strengthen when interval of gaps increases, when interval of gaps is in the same magnitude with incoming wave, the equalizing value of three-gap plan increases about 15dB , scattering curve surges more intensively in the nearby of this fixed value when D increases. The interval of gaps influent the space distribution of multi-gaps scattering and the position of its peak value greatly, scattering of each gap is independent through analyzing, these gaps make different overlap effect (increase or decrease) while being overlapped to be all field because of their different pitching

angle (the change of the phase position of each gap).

3.3 Analysis of gap scattering characteristic

3.3.1 Scattering characteristic of single gap

(1) Scattering strengthens when the width of single gap increases. When width is less than $1/4$ of incoming wave, scattering strengthens more rapidly when width increases; When width is larger than $1/4$ of incoming wave, scattering strengthens correspondingly gently when width increases.

(2) Scattering curves become flat when width of single gap increases. When a is relatively small, scattering curves are flat, when a is relatively large, peak values emerge in the nearby of $\pm 70^{\circ}$ when it is in near paralleling incidence direction.

3.3.2 Scattering characteristic of multi-gaps

(1) Mutual coupling. Scattering of single-gap plate behaves as flat curves, but the coupling of multi-gaps behaves as surging in intensity, but the increment of equalizing value is correspondingly in accord with single gap.

(2) Scattering behaves as the equalizing value of RCS is correspondingly unchanged, but when D increases, the surging strengthens.

Which should be noticed is that the scattering characteristic of single gap and multi-gaps in VV polarization is similar with that of HH polarization, the RCS value and its increment comparing to flat plate in HH polarization are large than that of VV polarization.

4 Analysis of steps scattering characteristic

4.1 Numerical calculating result of single step

The calculating model of single step is similar with that of single gap, it only needs to change the gap into step at the same position on plate. Correspondingly $R=9$, it is in resonance region, depth is 5mm , height of step h is separately $1\text{mm}, 1.5\text{mm}, 2\text{mm}$, depth of the thinner side is separately $4\text{mm}, 3.5\text{mm}, 3\text{mm}$,

influence laws to RCS which are caused by the height of single step is the main research target.

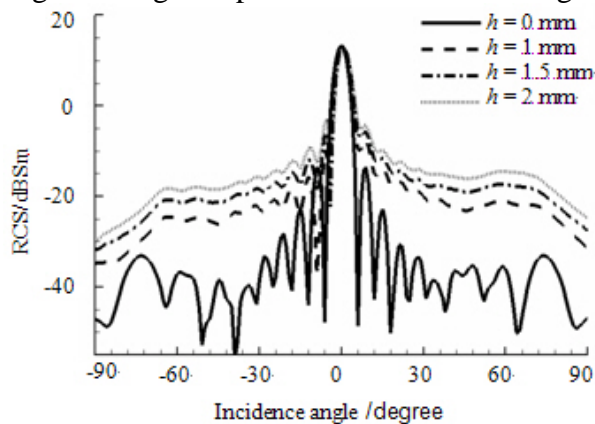


Fig. 6 RCS calculating curves of different height single step

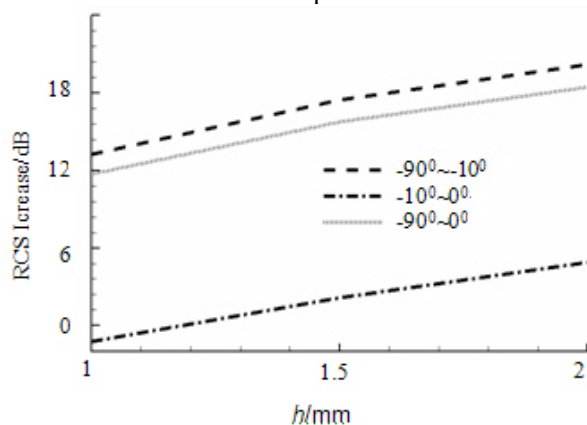


Fig. 7 RCS increase in different angle zone when height of single step changes

Fig.6 is RCS curves of different height of single step when their pitching angles to incoming wave change with time. Fig.7 exhibits the RCS acceleration of different height single-step plates comparing to flat plate in following different angle zone: $-90^{\circ}\sim-10^{\circ}$ 、 $-10^{\circ}\sim-0^{\circ}$ 、 $-90^{\circ}\sim-0^{\circ}$.

It could be told from fig.6 that scattering of single-step plate is obviously stronger than flat plan, its RCS curve shows a weak diagonal character, scattering from the thinner side of plan is relatively weaker. In HH polarization condition, RCS curves is gentle in $\pm 10^{\circ}\sim\pm 60^{\circ}$ scope, when height of single step keeps increasing, scattering of single step strengthen markedly, shows a straight up trend.

Because of the diagonal character of RCS curve, Fig.7 shows only the increment of equalizing value in $-90^{\circ}\sim-0^{\circ}$ zone. It exhibit that equalizing value increases along with the increasing of height, which means scattering of

single step strengthen along with the increasing of height; the increment of RCS is the largest in $-90^{\circ}\sim-10^{\circ}$ zone, which is followed by that in $-90^{\circ}\sim-0^{\circ}$ zone.

When incoming angle is in $\pm 10^{\circ}$ zone, scattering mainly performs as mirror scattering, the influence from single step is weak, it could be neglected in such situation; when in $-10^{\circ}\sim-60^{\circ}$ 、 $10^{\circ}\sim 60^{\circ}$ zone, scattering of single-step plate is stronger than flat plate, the difference between them is mainly caused by the scattering of single step itself, the scattering intensity and the shape of scattering curve change obviously according to the difference of step height and polarization, it performs as scattering strengthens markedly along with the increasing of step height; when in $-60^{\circ}\sim-90^{\circ}$ 、 $60^{\circ}\sim 90^{\circ}$ zone, it is in near paralleling incidence direction, its influence could be told at the edge of RCS curves.

4.2 Numerical calculating result of three steps

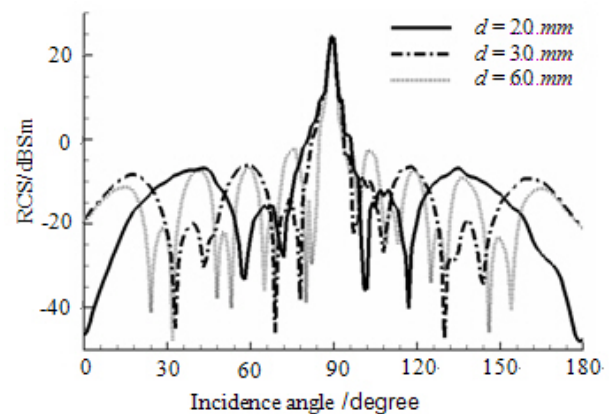


Fig. 8 RCS calculating curves of different interval of three steps

The exact structure of three-step plate is similar with three-gap plate, it only need to change gaps into steps in the same position on plate, steps go straight to the edges of plate, correspondingly $R=19$, it is in high frequency zone, Fig.8 shows the calculating RCS curves of three-step plate when separately $d=20, 30, 60$ mm, correspondingly $D=0.6, 1, 2$, it could be told from this result that, similar with three-gap plate, steps influent scattering greatly, and also surge in the nearby of -20 dBsm, the surging becomes more intensively when interval of

steps increases. Fig.12 shows that, in same step height condition, equalizing values of three-step plates are all about 17dB when the interval of steps is in the same magnitude with incoming wave, surging of scattering curves strengthen intensively along with the increasing of D , it could be explained with that the coupling effect between steps performs mainly as the surging of RCS curve when interval of steps increase.

4.3 Analysis of steps scattering characteristic

4.3.1 Scattering characteristic of single step

(1) Scattering shows a weak diagonal character. It is diagonal with 0^0 position, scattering of thinner side of plate is correspondingly weaker, RCS curves are relatively gentle in a big angle scope, scattering changes more intensively along with the increasing of step height, especially in $-60^0 \sim -90^0$ 、 $60^0 \sim 90^0$ zone.

(2) Scattering strengthens when step height increases. Refer to 1mm step height, scattering increases in a small level, its increment equalizing value is 11.71dB, step scattering increasing rapidly, refer to 2mm step height, increment equalizing value is the largest, to 18.47dB.

4.3.2 Scattering characteristic of multi-steps

Besides having the same scattering characteristic of single step, multi-steps was proved to also have the following characteristic by calculating:

(1) Mutual coupling. Single-step plate performs as flat curve, but multi-steps performs as intensive surging because of the coupling between steps, scattering of each step is independent through analyzing, these steps make different overlapped effect while being overlapped to be all field because of their different pitching angle (the change of the phase position of each gap), but its equalizing value is in accord with single step.

(2) Scattering behaves as the equalizing value of RCS is correspondingly unchanged when interval of steps is in the same magnitude with incoming wave, but along with the increasing of D , the surging strengthens.

Besides, similar with gap scattering characteristic, the RCS value and its increment comparing to flat plate in HH polarization are large than that of VV polarization.

5 Conclusions

Through comparing the result of experimentation of three gaps to the result of its calculating curves, the feasibility of procedure developed in this paper in analyzing of discrete characteristic of stealth aircraft is proved. The scattering characteristic of single gap, single step, three gaps, three steps in resonance region ($R=9$) and high frequency region ($R=19$) has been calculated and analyzed in this paper, the laws of gap scattering which are caused by gap width, gap interval, polarization and the laws of step scattering which are caused by step height, step interval, polarization have been researched, and through analyzing to get the primary laws of the relationship between single gap and three gaps and the relationship between single step and three steps: scattering of single gap strengthens along with the increasing of gap width, scattering of single step strengthens along with the increasing of step height; scattering of three gaps and three steps both have the coupling character, surging of RCS curves strengthens along with the increasing of intervals, it could be understood as the effect of mutual coupling; increment of RCS equalizing value in HH polarization is stronger than that of VV polarization. This result is significant to stealth aircraft designs, it could be taken as methods of stealth design technologies to strengthen its stealth ability.

Copyright Statement

We confirm that we, and our institution, hold copyright on all of the original material included in our paper. We also confirm we have obtained permission, from the copyright holder of any third party material included in our paper, to publish it as part of our paper. We grant full permission for the publication and distribution of our paper as part of the ICAS2008 proceedings or as individual off-prints from the proceedings.

References

- [1] Rao S M, Wilton D and Glisson A. Electromagnetic scattering by surfaces of arbitrary shape. *IEEE Transaction on Antennas Propagation*, Vol. 30, No. 5, pp 409-418, 1982
- [2] Song J M, Chew W C. Fast multipole method solution of three dimensional integral equation. *IEEE Transaction on Antennas Propagation*, Vol. 45, No. 10, pp 1528-1531, 1995
- [3] Song J M, Lu C C and Chew W C, et al. Fast illinois solver code (FISC). *IEEE Antennas and Propagation Magazine*, Vol. 40, No. 3, pp 27-341, 1998
- [4] Song J M, Chew W C. Error anlysis for the truncation of multipole expansion of vector Green's function[J]. *IEEE Microwave and Wireless Components Letters*, Vol. 11, No. 7, pp 311-313, 2001